New P-Type of Poly(4-methoxy-triphenylamine)s Derived by Coupling Reactions: Synthesis, Electrochromic Behaviors, and Hole Mobility

HUI-WEN CHANG,[1] KAI-HAN LIN,[2] CHU-CHEN CHUEH,[3] GUEY-SHENG LIOU,[1] WEN-CHANG CHEN[1,3]

[1]Institute of Polymer Science and Engineering, National Taiwan University, 1 Roosevelt Road, 4th Sec., Taipei 10617, Taiwan

[2]Department of Applied Chemistry, National Chi Nan University, 1 University Road, Puli, Nantou Hsien 545, Taiwan

[3]Department of Chemical Engineering, National Taiwan University, 1 Roosevelt Road, 4th Sec., Taipei 10617, Taiwan

Received 3 March 2009; accepted 8 April 2009
DOI: 10.1002/pola.23465
Published online in Wiley InterScience (www.interscience.wiley.com).

ABSTRACT: Methoxy-substituted poly(triphenylamine)s, poly-4-methoxytriphenylamine (**PMOTPA**), and poly-*N*,*N*-bis(4-methoxyphenyl)-*N*′,*N*′-diphenyl-*p*-phenylenediamine (**PMOPD**), were synthesized from the nickel-catalyzed Yamamoto and oxidative coupling reaction with $FeCl_3$. All synthesized polymers could be well characterized by ^1H and ^{13}C NMR spectroscopy. These polymers possess good solubility in common organic solvent, thermal stability with relatively high glass-transition temperatures (T_gs) in the range of 152–273 °C, 10% weight-loss temperature in excess of 480 °C, and char yield at 800 °C higher than 79% under a nitrogen atmosphere. They were amorphous and showed bluish green light (430–487 nm) fluorescence with quantum efficiency up to 45–62% in NMP solution. The hole-transporting and electrochromic properties are examined by electrochemical and spectroelectrochemical methods. All polymers exhibited reversible oxidation redox peaks and E_{onset} around 0.44–0.69 V versus Ag/AgCl and electrochromic characteristics with a color change under various applied potentials. The series of **PMOTPA** and **PMOPD** also showed p-type characteristics, and the estimated hole mobility of **O-PMOTPA** and **Y-PMOPD** were up to 1.5×10^{-4} and 5.6×10^{-5} $cm^2\ V^{-1}\ s^{-1}$, respectively. The FET results indicate that the molecular weight, annealing temperature, and polymer structure could crucially affect the charge transporting ability. This study suggests that triphenylamine-containing conjugated polymer is a multifunctional material for various optoelectronic device applications. © 2009 Wiley Periodicals, Inc. J Polym Sci Part A: Polym Chem 47: 4037–4050, 2009

Keywords: electrochemistry; electrochromic; fluorescence; functionalization of polymers; hole-moblity; luminescence; polyamines; poly(triphenylamine)s

INTRODUCTION

Conjugated polymers have shown potential applications in different electronic and optoelectronic devices, such as electroluminescence displays,[1–3] photovoltaic devices,[4] and thin film transistors.[5]

Additional Supporting Information may be found in the online version of this article.

Correspondence to: G.-S. Liou (E-mail: gsliou@ntu.edu.tw) or W.-C. Chen (E-mail: chenwc@ntu.edu.twedu.tw)

Journal of Polymer Science: Part A: Polymer Chemistry, Vol. 47, 4037–4050 (2009)

They are mechanically flexible, fabricated in large areas, and patterned with relative ease by casting the semiconducting and luminescent polymer from solution, and the color of the emitted light can be tailored by various chemical modification of the molecular structure. Generally, conjugated polymers were prepared by several methods (Stille, Yamamoto, Suzuki, Oxidative couplings, etc.)[6–9] to acquire highly pure polymers with optimized physical properties. For instance, the synthesis of well-defined polyacetylene,[10] polythiophenes,[11] polyphenylenes,[12] polyfluorenes,[13] ladder-conjugated polymers,[14] and other aromatic polymers[15] have led to a significant improvement in the performance of these polymeric materials and a better understanding of their structure-property relationships. However, the solubility of many highly conjugated polymers is low, particularly for blue-emitting species. Therefore, these targeted blue emitting polymers were often designed to bear large alkyl, alkoxy, or aryloxy groups to improve solubility and thus lower their glass transition temperatures (T_gs) and thermal stability. To obtain high T_g polymers, incorporating triphenylamine (TPA) units into the polymer main chain is a feasible approach. Ogino et al. have successfully prepared TPA-containing polymers having hole-transporting ability.[16,17] Kakimoto et al.[18,19] also reported that the charge injection and electroluminescent efficiency were improved remarkably by the incorporation of the hole-transporting TPA moieties into the polyimide backbone.

Triphenylamine and its derivatives are well-known hole transport materials in organic photoelectronic devices due to their ability to form stable radical cations and high drift mobility.[20–25] The combination of TPA with linear π-conjugated systems could be expected to lead to amorphous materials with isotropic optical and charge-transport properties.[26] In addition, the incorporation of bulky and three-dimensional TPA moiety into the polymer backbone leads to good solubility in many aprotic solvents and exhibited excellent thin-film-forming capability. The amorphous character of these materials offers the possibility to develop organic semiconductors with isotropic optical and charge-transport properties. We have demonstrated that TPA derivatives exhibited lower oxidation potential and the resulted TPA cation radical could be stabilized when electrodonating groups (methyl, methoxy) substituted at the para-phenyl positions.[27] Triphenylamine (TPA) based polymers are not only widely used as the hole-transport layer in electroluminescent devices but also show interesting anodic electrochromic behavior. One of the interesting multicolor systems is based upon the *N,N,N′,N′*-tetraphenyl-*p*-phenylenediamine moiety.[28,29] For the past decades, intramolecular electron transfer (ET) and electronic coupling effects in the oxidized states have been studied extensively in mixed-valence (MV) systems[30–33] and were utilized to design of new *N,N,N′,N′*-tetraphenyl-*p*-phenylenediamine-based polymers for electrochromic devices.[30] The properties of one-dimensional MV compounds containing two or more redox states connected via σ- or π-bridge molecule depend strongly on the extent of electronic interaction between the redox centers. An experimental and theoretical study of the *N,N,N′,N′*-tetraphenyl-*p*-phenylenediamine cation radical has been reported recently, and a symmetrical delocalized class III structure (with strong electronic coupling and the electron is delocalized over the two redox centers) was proposed in accordance to the Robin-Day classification.[34,35] The redox properties, ion-transfer process, electrochromism, and photoelectrochemical behavior of *N,N,N′,N′*-tetrasubstituted-1,4-phenylenediamine are important for technological applications.[36,37]

In this article, we report the two distinct synthetic approaches to prepare a series soluble TPA-based conjugated polymers with electro-donating methoxy substituted at the para-phenyl positions, which not only could prevent coupling reactions by affording stable cationic radicals but also lower their oxidation potentials. Some properties of polymer could be improved by increasing of molecular weight, include the possibility of extended p-conjugation, higher glass transition temperature (T_g), excellent film-forming property, and stable film morphology. For the purpose, the **O-PMOTPA** with higher molecular weight could be obtained by the simply chemical oxidative polymerization using ferric chloride as catalyst. The general properties such as solubility and thermal properties are described. The electrochemical, electrochromic, photoluminescent, and field-effect transistor (FET) properties of the polymers were also investigated herein and compared the resulted polymers from different synthetic method.

EXPERIMENTAL

Materials

4-Methoxytriphenylamine (**MOTPA**) (mp: 108–110 °C; lit.[38]: 108–110 °C by DSC at 10 °C/min)

and *N,N*-bis(4-methoxyphenyl)-*N′,N′*-diphenyl-*p*-phenylenediamine (**MOPD**) (mp: 97–98 °C; lit.[24]: 100–104 °C by DSC at 10 °C/min) were synthesized from 4-iodoanisole with diphenylamine and *N,N′*-diphenyl-*p*-phenylenediamine, respectively, by Ullmann condensation according to the previous studies.[23] 4-Methoxy-*N,N*-bis(4-bromophenyl)aniline (**DBrMOTPA**) was prepared according to the published procedures[39] by reaction with *N*-bromosuccinimide (NBS) (99%, ACROS). Diphenylamine (99%, ACROS), plladium on charcoal (Pd/C) (FLUKA), sodium hydride (95%; dry ALDRICH), 4-iodoanisole (98%, ACROS), copper powder (99%, ACROS), potassium carbonate (SCHARLAU), triethyleneglycol dimethyl ether (TEGDME) (99%, ALFA AESAR), *N*-methyl-2-pyrrolidinone (NMP) (TEDIA), *N,N*-dimethylacetamide (DMAc) (TEDIA), chloroform ($CHCl_3$) (TEDIA), and tetrahydrofuran (THF) (TEDIA) were used without further purification. Zinc (ACROS), triphenylphosphine (ACROS), 2,2′-bipyridine (ACROS), and nickel chloride (STREM) were purified according to previously reported procedures.[40] Tetrabutylammonium perchlorate (TBAP) was obtained from TCI and recrystallized twice from ethyl acetate and then dried *in vacuo* before use. All other reagents were used as received from commercial sources.

N,N-*Bis(4-methoxyphenyl)*-N′,N′-*diphenyl*-p-*phenylenediamine (MOPD)*

A mixture of 4-aminotriphenylamine (3.90 g, 15 mmol), 4-iodoanisole (8.66 g, 37 mmol), copper powder (2.03 g, 32 mmol), potassium carbonate (8.56 g, 62 mmol), and triethyleneglycol dimethyl ether (TEGDME) (20 mL) was heated with stirring at 160 °C for 48 h and then precipitated into 700 mL of ice water. Recrystallization from hexane yielded 3.47 g of the desired compound (**MOPD**) as dirt yellow powder in 49% yield; mp: 100–104 °C; Anal. Calcd for $C_{32}H_{28}N_2O_2$ (472.58): C, 81.33%; H, 5.97%; N, 5.93%. Found: C, 81.28%; H, 5.56%; N, 5.86%. ^{1}H NMR (DMSO-d_6, ppm): 3.71 (s, 6H, OCH_3), δ 6.76 (d, 2H), δ 6.87–7.01 (m, 16H), δ 7.24 (t, 4H); ^{13}C NMR (DMSO-d_6, ppm): 55.4, 115.08, 121.43, 122.20, 122.71, 126.30, 126.50, 129.50, 139.93, 140.55, 144.72, 147.65, 155.62.

N,N-*Bis(4-methoxyphenyl)*-N′,N′-*bis(4-bromophenyl)*-p-*phenylenediamine (DBrMOPD)*

N,N-Bis(4-methoxyphenyl)-*N′,N′*-diphenyl-*p*-phenylenediamine (**MOPD**) (2.84 g, 6.0 mmol) and *N*-bromosuccinimide (NBS) (2.31 g, 13 mmol) were fully dissolved in DMF. The predissolved NBS solution was dropped in to the solution of **MOPD** slowly in the ice bath. The mixture solution then stirred at room temperature for 48 h under nitrogen atmosphere. The reaction mixture was added to 150 mL of water in a separatory funnel. The precipitate was collected, purified by reflux in ethanol for 30 min, and then filtered and dried *in vacuo* at 80 °C for 24 h to acquire the final product (**DBrMOPD**); yield: 60%; mp 202–203 °C; Anal. Calcd for $C_{32}H_{26}Br_2N_2O_2$ (630.36): C, 60.97%; H, 4.16%; N, 4.44%. Found: C, 60.60%; H: 4.33%; N: 4.17%. ^{1}H NMR (DMSO-d_6, ppm): 3.72 (s, 6H, OCH_3), δ 6.75 (d, 2H), δ 6.88 (m, 10H), δ 7.00 (d, 4H), δ 7.41 (d, 2H); ^{13}C NMR (DMSO-d_6, ppm): 55.2, 113.78, 114.96, 120.59, 124.23, 126.55, 126.85, 132.18, 138.27, 140.07, 145.46, 146.40, 155.71.

Polymer Synthesis

Polymerization via Yamamoto Coupling

Poly-4-methoxytriphenylamine (**Y-PMOTPA**) and poly-*N,N*-bis(4-methoxyphenyl)-*N′,N′*-diphenyl-*p*-phenylenediamine (**Y-PMOPD**) were prepared by Yamamoto coupling with $NiCl_2$ as catalyst from **DBrMOTPA** and **DBrMOPD**, respectively. All the reactions were carried out under dry nitrogen atmosphere using anhydrous DMAc as solvent. The synthesis of polymer **Y-PMOPD** is used as an example to illustrate the general synthetic route. The typical procedure is as follows. In a 50-mL round-bottomed flask, $NiCl_2$ (27.22 mg, 0.21 mmol), PPh_3 (1.30 g, 4.20 mmol), 2,2′-bipyridine (32.80 mg, 0.21 mmol), zinc (0.85 g, 13.00 mmol), monomer **DBrMOPD** (1.89 g, 3.00 mmol), and anhydrous DMAc (3 mL) were placed under nitrogen. The mixture was stirred at 80 °C for 24 h and poured into a mixture of methanol containing 10% hydrochloric acid. Then reprecipitations of the filtered crude polymers from $CHCl_3$ into methanol were carried out twice for further purification, followed by drying *in vacuo*. The resulting polymer **Y-PMOPD** is a greenish yellow powder with highly yield (91%); ^{1}H NMR (chloroform-*d*, δ, ppm): 3.79 (s, OCH_3), 6.81 (d, 4H), 6.88–7.02 (m, 4H), 7.06 (d, 4H), 7.14 (d, 4H), 7.44 (d, 4H); ^{13}C NMR (chloroform-*d*, δ, ppm): 55.5, 114.6, 122.1, 123.3, 126.1, 127.1, 128.9, 134.2, 140.4, 141.2, 144.6, 146.7, 155.5. **Y-PMOTPA** was synthesized by a similar procedure as described earlier. The color of **Y-PMOTPA** powder is

yellowish green (yield: 84%); ^{1}H NMR (chloroform-*d*, δ, ppm): 3.76 (s, OCH_3), 6.85 (m, 6H), 6.94 (t, 2H), 7.04–7.14 (m, 18H), 7.21 (t, 4H), 7.41 (m, 8H); ^{13}C NMR (chloroform-*d*, δ, ppm): 55.5, 114.8, 122.0, 122.9, 123.0, 127.1, 127.3, 129.1, 134.0, 134.1, 140.5, 140.6, 146.8, 147.0, 148.0, 156.2.

Polymerization via Oxidative Coupling

Poly-4-methoxytriphenylamine (**O-PMOTPA**) was synthesized as follows. To a two-necked 50 mL flask equipped with a magnetic stirrer were placed **MOTPA** (3 mmol) and chloroform (3 mL) under nitrogen atmosphere. A quarter portion of $FeCl_3$ (3 mmol; total is 12 mmol) was added to the reaction mixture at the interval of 1 h. The solution was stirred at 45 °C for 24 h and poured into a mixture of methanol containing 10% hydrochloric acid to recover the product. Collected powder was dissolved in chloroform and reprecipitated with acetone containing small amount of aqueous ammonia. The resulting polymer was filtered and dried *in vacuo* at 100 °C for 24 h (yield: 85%).

Preparation of Polymer Film

A solution of polymer was made by dissolving about 0.5 g of the polymer sample in 10 mL of $CHCl_3$. The homogeneous solution was poured into a 9-cm glass Petri dish, which was placed in the atmosphere for 8 h to remove most of the solvent; then the semidried film was further dried *in vacuo* at 100 °C for 4 h. The obtained films were about 50–70 μm in thickness and were used for molecular weights measurements, solubility tests, and thermal analyses.

Organic Field Effect Transistor Fabrication

The organic field effect transistors (OFETs) of **PMOTPA** series and **PMOPD** were fabricated through the bottom-contact and bottom-gate geometry. A thermally grown 200 nm SiO_2 on the p-doped silicon wafers used as the gate dielectric with a capacitance of 17 nF/cm^2. The aluminum was used to create a common bottom-gate electrode. The source/drain regions were defined by a 130 nm Au through a regular shadow mask, and the channel length (L) and width (W) were 25 and 500 μm, respectively. Afterward, the substrate was modified with octyltrichlorosilane (OTS) as silane coupling agents. 0.5 wt % polymer solutions in chloroform were filtered through 0.45 μm pore size PTFE membrane syringe filters, spin-coated at a speed rate of 1000 rpm for 60 s onto the silanized SiO_2/Si substrate and annealed at 100 °C or above T_g for 3 h, except for **O-PMOTPA**, under vacuum. Output and transfer characteristics of the OTFT devices were measured using a Keithley 4200 semiconductor parametric analyzer. All the electronic measurements were performed in ambient atmosphere.

Measurements

^{1}H and ^{13}C NMR spectra were measured on a Bruker Avance 300 MHz FT-NMR system. Elemental analyses were run in an Elementar VarioEL-III. Gel permeation chromatography (GPC) was carried out on a Waters chromatography unit interfaced with a Waters 2410 refractive index detector. Two Waters 5 μm Styragel HR-2 and HR-4 columns (7.8 mm I. D. $\times$ 300 mm) were connected in series with *N*-methyl-2-pyrrolidinone (NMP) as the eluent at a flow rate of 1 mL/min and were calibrated with narrow polystyrene standards. Ultraviolet–visible (UV–vis) spectra of the polymer films were recorded on a Varian Cary 50 Probe spectrometer. Thermogravimetric analysis (TGA) was conducted with a PerkinElmer Pyris 1 TGA. Experiments were carried out on ~6–8 mg film samples heated in flowing nitrogen or air (flow rate = 40 cm^3/min) at a heating rate of 20 °C/min. DSC analyses were performed on a PerkinElmer Pyris Diamond DSC at a scan rate of 20 °C/min in flowing nitrogen (20 cm^3/min). Electrochemistry was performed with a CHI 611B electrochemical analyzer. Voltammograms are presented with the positive potential pointing to the left and with increasing anodic currents pointing downwards. Cyclic voltammetry was performed with the use of a three-electrode cell in which ITO (polymer films area about 0.7 cm $\times$ 0.5 cm) was used as a working electrode. A platinum wire was used as an auxiliary electrode. All cell potentials were taken with the use of a homemade Ag/AgCl, KCl (sat.) reference electrode. Absorption spectra in the spectroelectrochemistry experiments were measured with a HP 8453 UV–visible spectrophotometer. Photoluminescence spectra were measured with a Jasco FP-6300 spectrofluorometer. Irradiation of the photochemical reaction system with light was also carried out by using Jasco FP-6300 as the source of light. Output and transfer characteristics of the OFET devices were measured using Keithley 4200 semiconductor parametric analyzer. All the prepared

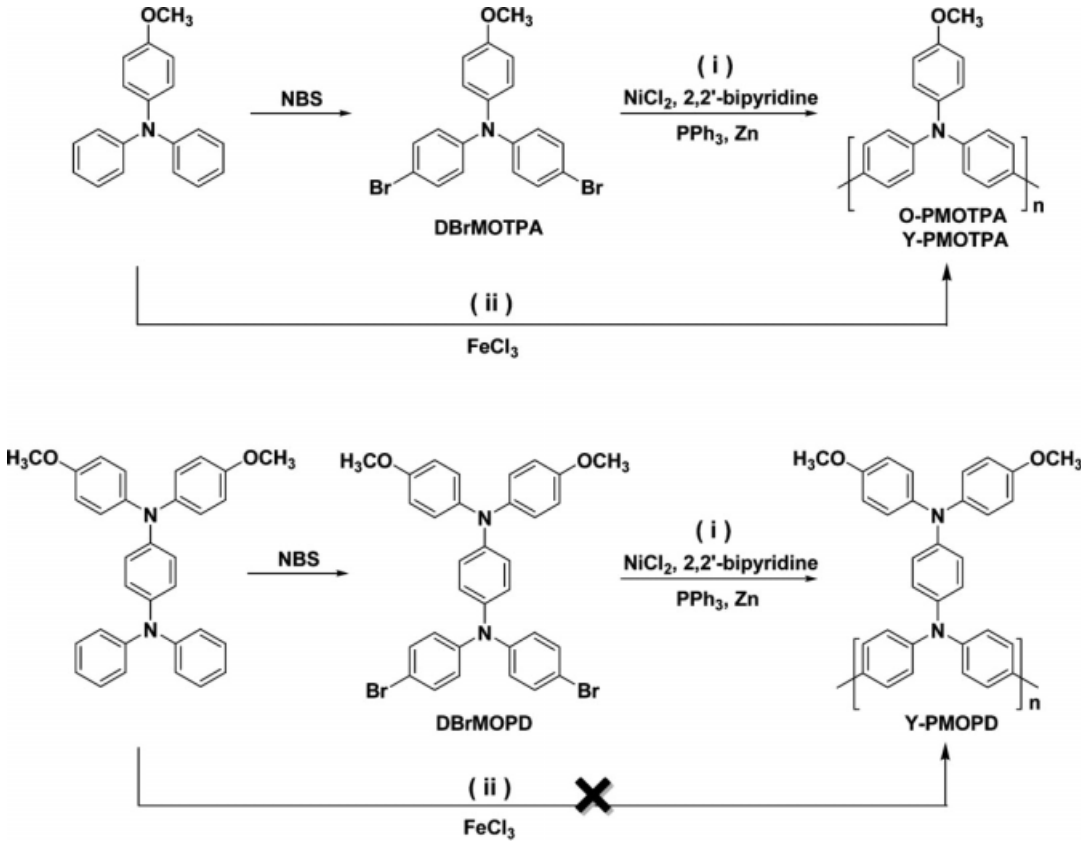

Scheme 1. Synthesis routes for **PMOTPA** series and **PMOPD**. (i) Synthesis of **Y-PMOTPA** and **Y-PMOPD** via Yamamoto coupling polymerization. (ii) Synthesis of **O-PMOTPA** via oxidative coupling polymerization.

procedures and electronic measurements are performed in ambient atmosphere. Atom force microscopy (AFM) measurements were obtained with a NanoScope IIIa AFM (Digital Instruments, Santa Barbara, CA) at room temperature. Commercial silicon cantilevers (Nanosensors, Germany) with typical spring constants of 21–78 N m^{-1} were used to operate the AFM in tapping mode. Images were taken continuously with the scan rate of 1.0 Hz.

RESULTS AND DISCUSSION

Synthesis and Characterization

The novel monomer (**DBrMOPD**) was synthesized through the bromination of **MOPD** with *N*-bromosuccinimide (NBS) as described in Scheme 1. It was obtained in a high yield and characterized by ^{1}H NMR, ^{13}C NMR as showed in Supporting Information Figure S1. Assignments of each carbon and proton are assisted by the two-dimensional H-H COSY and C-H HMQC NMR spectrum shown in Supporting Information Figures S2 and S3, and these spectra agree well with the proposed molecular structure of **DBrMOPD**. The organo-soluble TPA-containing aromatic polymers, poly-4-methoxy-triphenylamine (**Y-PMOTPA**) and poly-*N*,*N*-bis(4-methoxyphenyl)-*N*′,*N*′-diphenyl-*p*-phenylenediamine (**Y-PMOPD**), could be readily prepared by palladium-catalyzed Yamamoto coupling polymerization. Moreover, the **O-PMOTPA** with a higher molecular weight could be acquired by simply oxidative coupling reaction, but in the case of polymerization of *N*,*N*-bis(4-methoxyphenyl)-*N*′,*N*′-diphenyl-*p*-phenylenediamine (**MOPD**), leaving only monomers at the end of polymerization. The results of no reaction in the case of **MOPD** can be explained by the fact that the **MOPD** have more radical of amino nitrogen could stabilize their resonance to reduce the reactivity.[41] The synthetic routes of the key monomer and target polymers were outlined in Scheme 1. The ^{1}H and ^{13}C NMR spectra of **Y-PMOTPA** and the corresponding monomer in $CDCl_3$ is showed in Supporting Information

Table 1. Basic Properties of Polymers

Polymer		Solvent[a]								
Code	η_{inh}[b] (dl/g)	NMP	DMAc	DMF	THF	$CHCl_3$	CH_3CN	Toluene	M_w[c]	PDI (M_n/M_w)
Y-PMOTPA	0.13	+ +	+	+	+ +	+ +	−	−	3,300	1.36
O-PMOTPA	0.39	+ +	−	−	−	+ +	−	−	43,700	3.25
Y-PMOPD	0.11	+ +	+ +	+	+ +	+ +	−	+ +	6,500	1.80

[a] Solubility: + +, soluble at room temperature; +, soluble on heating; −, insoluble even on heating.
[b] Measured at a polymer concentration of 0.5 g/dL in NMP at 30 °C.
[c] Values estimated by GPC using NMP as an eluent (polystyrene standards).

Figure S4. The ^1H NMR chemical shifts of the polymer are similar to those of the corresponding monomer but the peak is broader and not well resolved. This is consistent with what had observed in conjugated polymer and its corresponding monomer reported in the literature.[42] The structural analysis of the **Y-PMOTPA** from NMR spectroscopy revealed exclusive 4′,4″-linkage between consecutive TPA repeat units on the polymer chains.

The solubility behavior of resulting conjugated polymers was tested qualitatively, and the results are summarized in Table 1. All polymers exhibited highly soluble in aportic solvent except for **O-PMOTPA** which resulted from high molecular weight. The solubility and electrochemical stability of the TPA-containing polymer could be enhanced by substituent effect when the electrodonating substituents were incorporated at the para-position of TPA repeat unit. These polymers prepared by Yamamoto coupling polymerization had weight-average molecular weights ranging from 3300 to 6500 against polystyrene standards and polydispersity (PDI) around 1.36–1.80 by gel permeation chromatography (GPC) analysis. Furthermore, the **O-PMOTPA** obtained from oxidative polymerization possessed a higher weight-average molecular weight up to 43,700 than that by Yamamoto coupling polymerization. The photo-oxidation of polymer proceeded through the reaction of the photo-excited polymer with $CHCl_3$ probably led to the higher molecular weight by oxidative polymerization.

Polymer Properties

Thermal Properties

The thermal properties of all the obtained polymers were investigated by TGA, TMA, and DSC are summarized in Table 2. Typical TGA curves of **O-PMOTPA** in both air and nitrogen atmospheres are shown in Figure 1. All the aromatic polymers exhibited good thermal stability with insignificant weight loss up to 400 °C in nitrogen. Their 10% weight-loss temperatures in nitrogen and air were recorded at 485–520 and 485–500 °C, respectively, and carbonized residue (char

Table 2. Thermal Properties of **PMOTPA** Series and **PMOPD**[a]

Polymer Code	T_g (°C)[b]	T_s (°C)[c]	T_d at 5% Weight Loss (°C)[d]		T_d at 10% Weight Loss (°C)[d]		Char Yield (wt %)[e]
			N_2	Air	N_2	Air	
Y-PMOTPA	193	200	470	470	520	500	72
O-PMOTPA	273	281	465	470	510	510	79
Y-PMOPD	152	167	400	455	485	485	70

[a] The polymer film sample were heated at 200 °C for 1 h before all the thermal analyses.
[b] Midpoint temperature of baseline shift on the second DSC heating trace (rate 20/min) of the sample after quenching from 300 °C.
[c] Softening temperature measured by TMA with a constant applied load of 10 mN at a heating rate of 10 °C/min.
[d] Decomposition temperature, recorded via TGA at a heating rate of 20 °C/min.
[e] Residual weight percentage at 800 °C in nitrogen.

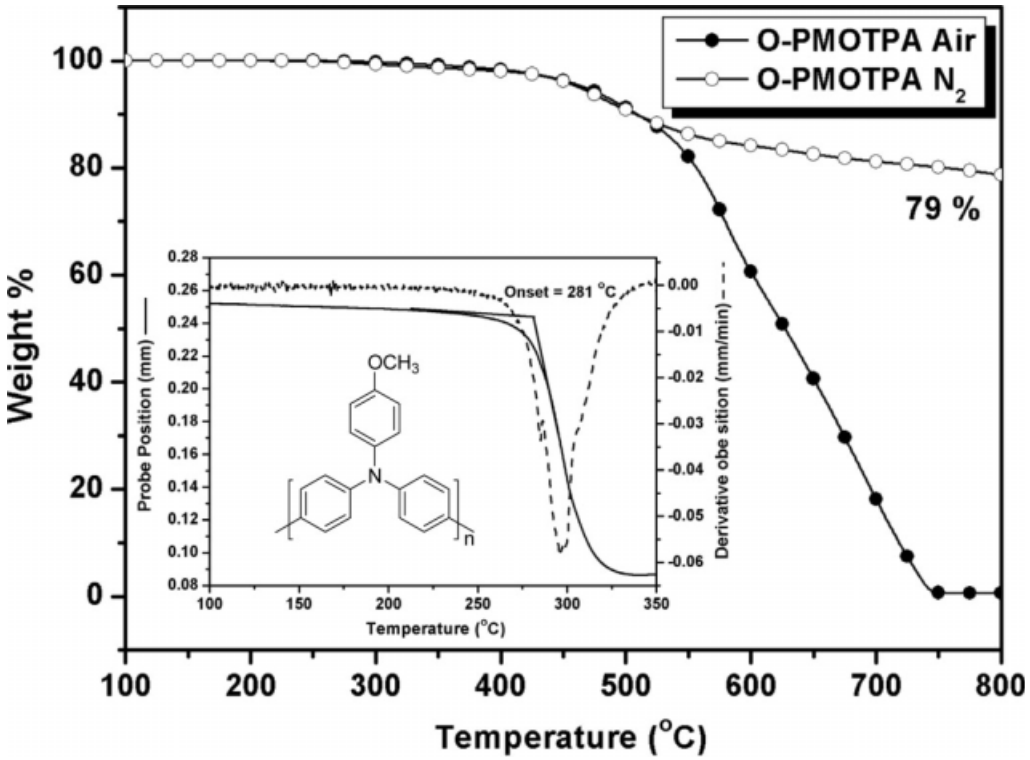

Figure 1. TGA and TMA curves for **O-PMOTPA** (TGA: at a scan rate of 20 °C/min; TMA: heating rate = 10 °C/min; applied force = 10 mN).

yield) of these aromatic polymers was more than 70% at 800 °C under nitrogen atmosphere. The high char yields of these polymers could be ascribed to their high aromatic content. The softening temperature (T_s) values of the polymer films were determined from the onset temperature of the probe displacement on the TMA trace. A typical TMA thermogram for **O-PMOTPA** is illustrated in Figure 1. The T_gs of all the polymers could be easily measured by the DSC thermograms; they were observed in the range of 152–273 °C could be easily measured by the DSC thermograms. All the polymers indicated no clear melting endotherms up to the decomposition temperatures on the DSC scans. This result also supports the amorphous nature of these TPA-containing polymers.

Optical and Electrochemical Properties

The electrochemical and optical properties of the polymers were investigated by cyclic voltammetry, UV–vis, and photoluminescence spectroscopy. The results are summarized in Table 3. The UV–vis absorption of 4-methoxy-substituted TPA-based polymers exhibited maximum absorption at 369–382 nm in NMP solution, due to the π-π^* transition resulting from the conjugation between the aromatic rings and nitrogen atoms. The photoluminescence emission maxima of the polymer solutions were around 430–487 nm with fluorescence quantum yield ranging from 23.6% for **Y-PMOPD** to 61.5% for **Y-PMOTPA**. The UV–vis absorption of these polymer films also showed similar maximum absorbance at 365–382 nm, indicating these polymers with bulky TPA units could be effectively restricted intermolecular packing and interactions. However, the absorption onset of the **PMOPD** films showed a red shift result than **PMOTPA** that could be attributed to the extended conjugation between the aromatic rings and nitrogen atoms through delocalization of π-electrons along the polymer backbone. Figure 2 illustrates the absorption and PL spectra of the solutions of Yamamoto coupling polymers in various solvents, as well as the spectra of its thin solid film. The absorption spectra of the four different solvents were very similar to each other, but the PL spectrum of **Y-PMOPD** progressively shifts to red with an increase in the solvent polarity, and PL emission maxima moving from 440 to 487 nm

Table 3. Optical and Electrochemical Properties of Polymers

Polymer Code	Solution λ (nm)[a]			Film λ (nm)			Oxidation (V) (vs. Ag/AgCl)					
	abs_{max}	PL_{max}[b]	Φ_{PL} (%)[c]	abs_{max}	abs_{onset}	PL_{max}[b]	First E_{onset}	First $E_{1/2}$	Second $E_{1/2}$	E_g (eV)[d]	HOMO (eV)[e]	LUMO (eV)[f]
Y-PMOTPA	381	430	61.5	379	430	458	0.67	0.86	–[g]	2.88	5.03	2.15
O-PMOTPA	382	431	26.3	376	428	447	0.69	0.93	–[g]	2.90	5.05	2.15
Y-PMOPD	369	487	23.6	365	435	461	0.44	0.57	1.02	2.85	4.80	1.95

[a] Polymer concentration of 10^{-5} M in NMP at room temperature.
[b] They were excited at abs_{max} for both solid and solution states.
[c] These values were measured by using 9,10-diphenylanrthance (dissolved in toluene with a concentration of 10^{-5} M, assuming FPL of 0.90) as a standard at 24–25 °C.
[d] The data were calculated by the equation: gap = $1240/\lambda_{onset}$ of polymer film.
[e] The HOMO energy levels were calculated from cyclic voltammetry and were referenced to ferrocene (4.8 eV).
[f] LUMO = HOMO-gap.
[g] –; No describe.

when the solvent is changed from toluene to NMP (summarized in Table 4). All the PL spectra of these polymers showed a blue shift when the solvent was changed from NMP to THF or chloroform. Generally, solvation should increase the interaction between polymer chain and solvent, which may consume certain excitation energy and lead to increase on the emission wavelength. On the other hand, the solvatochromic shifts occur merely in their emission spectra less than absorption spectra, implying that the excited-state energy levels are influenced more than those in the electronic ground state. The emission color also changes from blue in toluene to bluish green in NMP when the polymer solutions are irradiated under a 365 nm UV lamp (Fig. 2), which accord with their PL spectra. Further, the quantum efficiency of these polymers generally decreases with increasing polarity of solvent except for chloroform. It is interesting to note that the original bluish green emission of the polymers decreased dramatically in intensity in chloroform solution, and this phenomenon was not observed in other solvents such as NMP, THF, and toluene; the color and emission properties of the polymer solutions remained unchanged even after UV irradiation. This phenomenon could be explained by the reaction between photogenerated TPA radical cation and the halogenated solvent as known for aromatic compounds containing the amino, hydroxy, and mercapto substituents in halogenated solvents.[43] Photochemical reactions of some π-conjugated polymers with $CHCl_3$ had also been studied by several research groups.[44,45] Such as photooxidation of π-conjugated poly(phenothiazine), Jenekhe[43] proposed a reaction process involving generation of phenothiazine radial cation and reaction of the radical cation with $CHCl_3$. This result could be attributed to the phenothiazine is a highly electron-donating unit, facilitating formation of the radial cation under irradiation with light. TPA is also an electron-donating unit, whose electron-donating ability is enhanced by introducing the electron-donating methoxy group at the p-position of TPA unit; on the basis of the reported results, consequently, similar formation of radical cation in PMOTPA and PMOPD under irradiation with light is conceivable. This photooxidation reaction between polymer and $CHCl_3$ as one of the possible conjecture for that the PL intensity quenching in the $CHCl_3$ solution of these polymer under UV irradiation.

The redox behavior was investigated with cyclic voltammetry conducted by the cast film on an ITO-coated glass substrate as working electrode in dry acetonitrile contains 0.1 M of TBAP as an electrolyte for **Y-PMOTPA**. Because of scanty adhesion between **Y-PMOPD** and ITO substrate, the electrochemical analysis was carried out in CH_2Cl_2 solution (5×10^{-4} M). The cyclic voltammograms for these polymers exhibited reversible oxidation redox couples at E_{onset} = 0.44–0.67 V showed in Figure 3. For **Y-PMOPD** in Figure 3(b), there are two reversible oxidation redox couples at $E_{onset} = 0.44$ ($E_{1/2} = 0.57$ V) and $E_{1/2} = 1.02$ V, respectively. The first electron removal for **Y-PMOPD** was assumed to occur at the N atom on the pendent 4,4′-dimethoxydiphenylamine groups to yield one stable delocalized radical cation, which is more electron-richer than

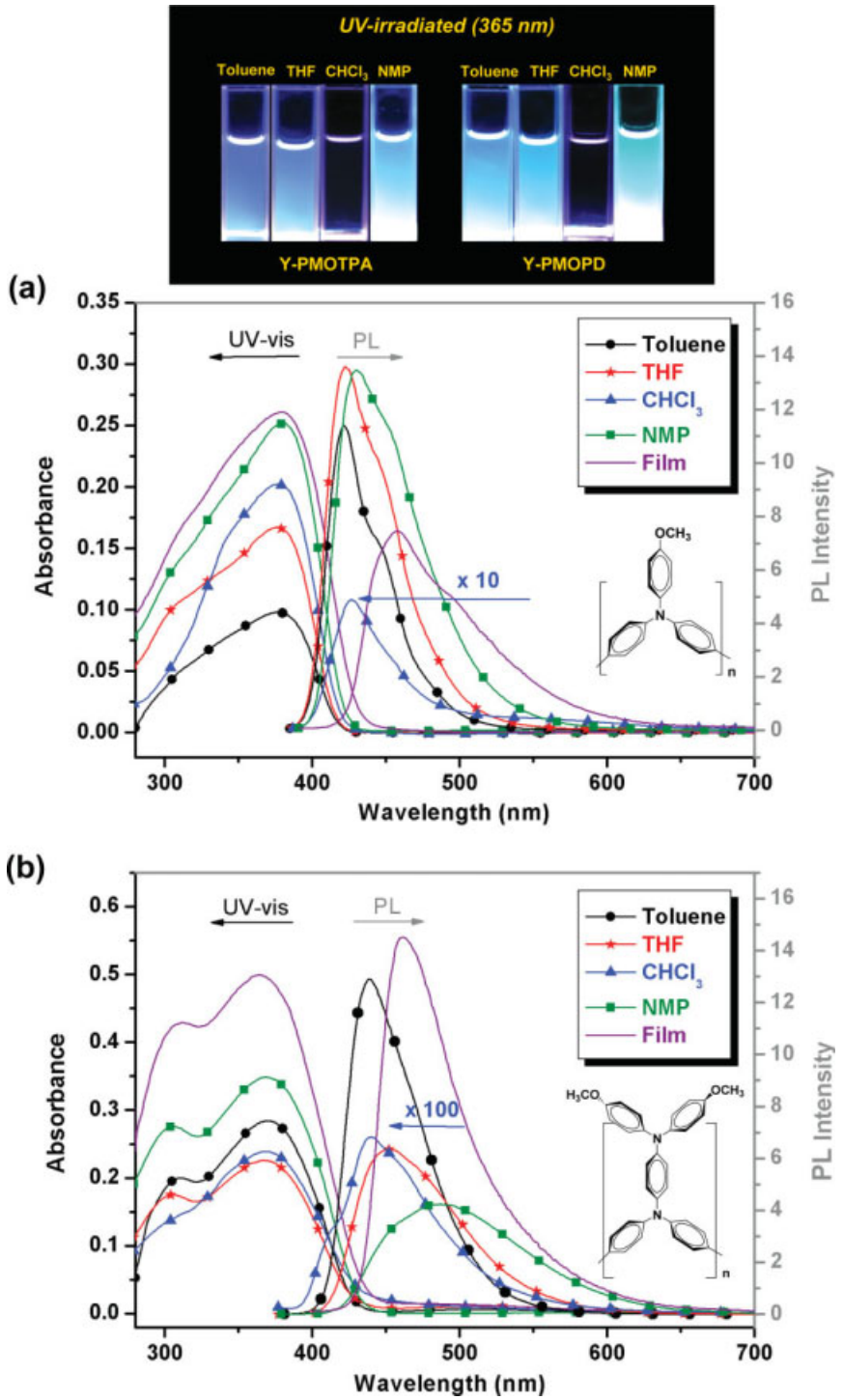

Figure 2. UV–vis and PL spectrums of (a) **Y-PMOTPA** and (b) **Y-PMOPD** in various solvents: NMP, $CHCl_3$, THF, and toluene at a concentration of 10^{-5} M, as well as its thin solid film. [Color figure can be viewed in the online issue, which is available at www.interscience.wiley.com.]

the N atom on the main chain TPA unit, and then further to form quinonoid-type dication with increasing applied potential. The energy of the highest occupied molecular orbital (HOMO) and lowest unoccupied molecular orbital (LUMO) levels of the investigated polymer could be

Table 4. Photophysical Properties of **Y-PMOTPA** and **Y-PMOPD** in Different Solvents[a]

	Y-PMOTPA			Y-PMOPD		
Solvent	λ_{abs} (nm)	$\lambda_{PL,\ max}$ (nm)	Φ_{PL} (%)[b]	λ_{abs} (nm)	$\lambda_{PL,\ max}$ (nm)	Φ_{PL} (%)[b]
Toluene	377	422	84.6	371	439	45.3
$CHCl_3$	377	427	2.5	367	440	0.4
THF	377	423	79.7	367	453	39.6
NMP	381	430	61.5	369	487	23.6

[a] The concentration of polymer was 10^{-5} M in different solvents.

[b] These values were measured by using 9,10-diphenylanrthance (dissolved in toluene with a concentration of 10^{-5} M, assuming FPL of 0.90) as a standard at 24–25 °C.

determined from their oxidation onset potentials and the onset absorption wavelength, and the results are listed in Table 3.

Electrochromic Characteristics

Electrochromic materials exhibit different colors depending upon the oxidation state, which was determined by optically transparent thin-layer electrode (OTTLE) coupled with a UV–vis spectroscopy. The electrode preparations and solution conditions were identical to those used in cyclic voltammetry. The typical electrochromic absorption spectra of **Y-PMOTPA** and **Y-PMOPD** are shown in Figures 4 and 5, respectively. In the neutral form, the film of **Y-PMOTPA** exhibited strong characteristic absorption of TPA at wavelength around 384 nm, which is almost transparent in the visible region. Upon oxidation (increasing applied potential from 0 to 0.90 V), the intensity of the absorption peak at 384 nm decreased gradually, while two new bands grew up at 495 and 696 nm, respectively. The color of the polymer was changed from neutral colorless to red (also

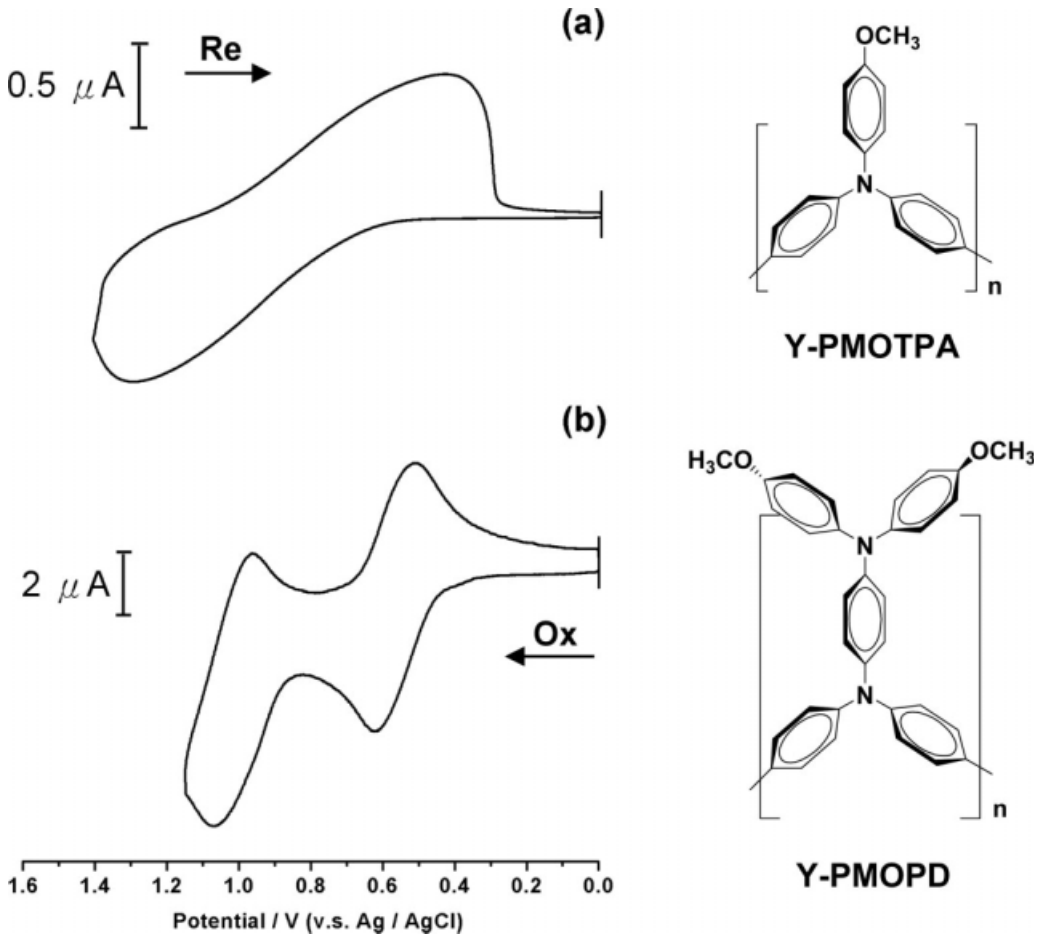

Figure 3. Cyclic voltammograms of (a) **Y-PMOTPA** film on an ITO-coated substrate in CH_3CN containing 0.1 M TBAP (b) the first and second oxidation redox of **Y-PMOPD** in CH_2Cl_2 solution (10^{-3} M) containing 0.1 M TBAP. Scan rate = 50 mV/s.

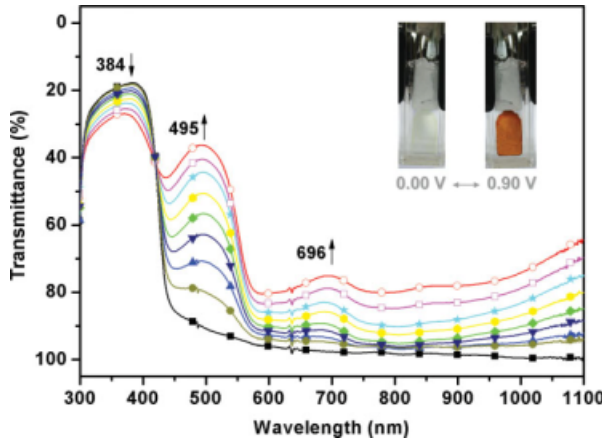

Figure 4. Electrochromic behavior of **Y-PMOTPA** thin film (in CH_3CN with 0.1 M TBAP as the supporting electrolyte) at 0.00 (■), 0.72 (●), 0.74 (▲), 0.77 (▼), 0.79 (◆), 0.82 (⬢), 0.84 (★), 0.87 (□), 0.90 V (○). [Color figure can be viewed in the online issue, which is available at www.interscience.wiley.com.]

shown in Fig. 4) with contrast of optical transmittance change ($\Delta T\%$) up to 54% at 495 nm. The electrochromic characteristic of **Y-PMOPD** shown in Figure 5 exhibited two coloration stages from the change of absorption spectra. When the applied potentials increased positively from 0.00 to 0.66 V during the first stage oxidation, the peak of absorption at 367 nm, characteristic for neutral form **Y-PMOPD** decreased gradually, while two new bands grew up at 425 and 1033 nm due to the formation of a stable monocation radical within the pendent 4,4′-dimethoxydiphenylamine moiety. When the potential was adjusted to a more positive value of 1.11 V, corresponding to the second step oxidation, the peak of characteristic absorbance decreased gradually while one new band grew up at 719 nm. This spectral change can be attributable to the formation of a dication in N atom between *para*-phenylenediamine units. Furthermore, the color of **Y-PMOPD** changed from green to blue with high contrast of optical transmittance change ($\Delta T\%$) up to 85% at 719 nm (as shown in Fig. 5).

Organic Field Effect Transistor Characteristics

Figure 6(a) showed the transfer characteristic curves of the **O-PMOTPA** and **Y-PMOPD** on OTS-modified SiO_2 and Figure 6(b) exhibited the output characteristic curve of the **O-PMOTPA** as a representative. The charge carrier mobility was calculated according to the transfer characteristic curves using the following eq 1. All the related OFET results are summarized in Table 5. The I–V curves showed that the **PMOTPA** and **PMOPD**-based thin-film transistor has the p-type characteristics with the accumulation operation. In the saturation region ($V_d > V_g - V_t$), the drain current I_d can be described by the following equation[46]:

$$I_d = \left(\frac{WC_o\mu_h}{2L}\right)(V_g - V_t)^2 \quad (1)$$

Where μ_h is the hole mobility, C_o is the capacitance of the gate insulator per unit area (SiO_2, 200 nm, $C_o = 17$ nF/cm^2), W is the channel width, L is the channel length, and V_t is the threshold voltage. The field-effect mobility of the saturation region was calculated from the transfer characteristics of the polymer devices. Furthermore, to clarify the carrier mobility mechanism, their morphology on the device surface was also investigated by AFM. Furthermore, to clarify the influence of annealing temperature on hole mobility, thermal treatment under two different temperatures was conducted, where one was below the T_g and the other was above the T_g. The saturated hole mobility of **Y-PMOTPA** (T_g: 193 °C), under 100 and 200 °C heat treatment is 5.0×10^{-5} and 9.0×10^{-5} cm^2 V^{-1} s^{-1} with the corresponding on/off ratios of 110 and 190. For the **O-PMOTPA** (T_g: 273 °C), the hole mobility under 100 and 275 °C heat treatment is 9.0×10^{-5} and 1.5×10^{-4} cm^2 V^{-1} s^{-1}, and their on/off ratios are

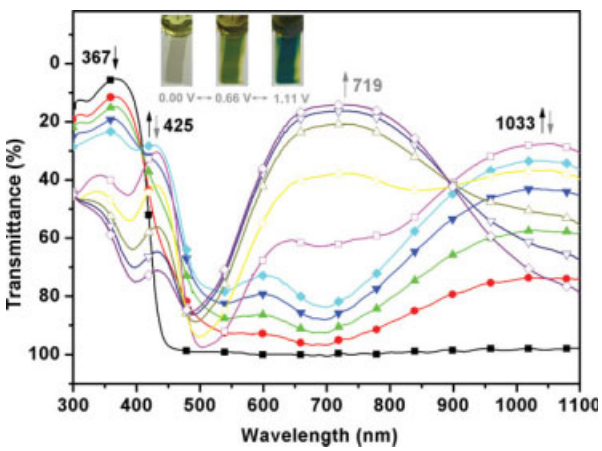

Figure 5. Electorchromic behavior of **Y-PMOPD** in CH_2Cl_2 solution (5×10^{-4} M) containing 0.1 M TBAP at 0.00 (■), 0.48 (●), 0.54 (▲), 0.60 (▼), 0.66 (◆), 0.93 (□), 0.96 (○), 0.99 (△), 1.02 (▽) and 1.11 (◇). [Color figure can be viewed in the online issue, which is available at www.interscience.wiley.com.]

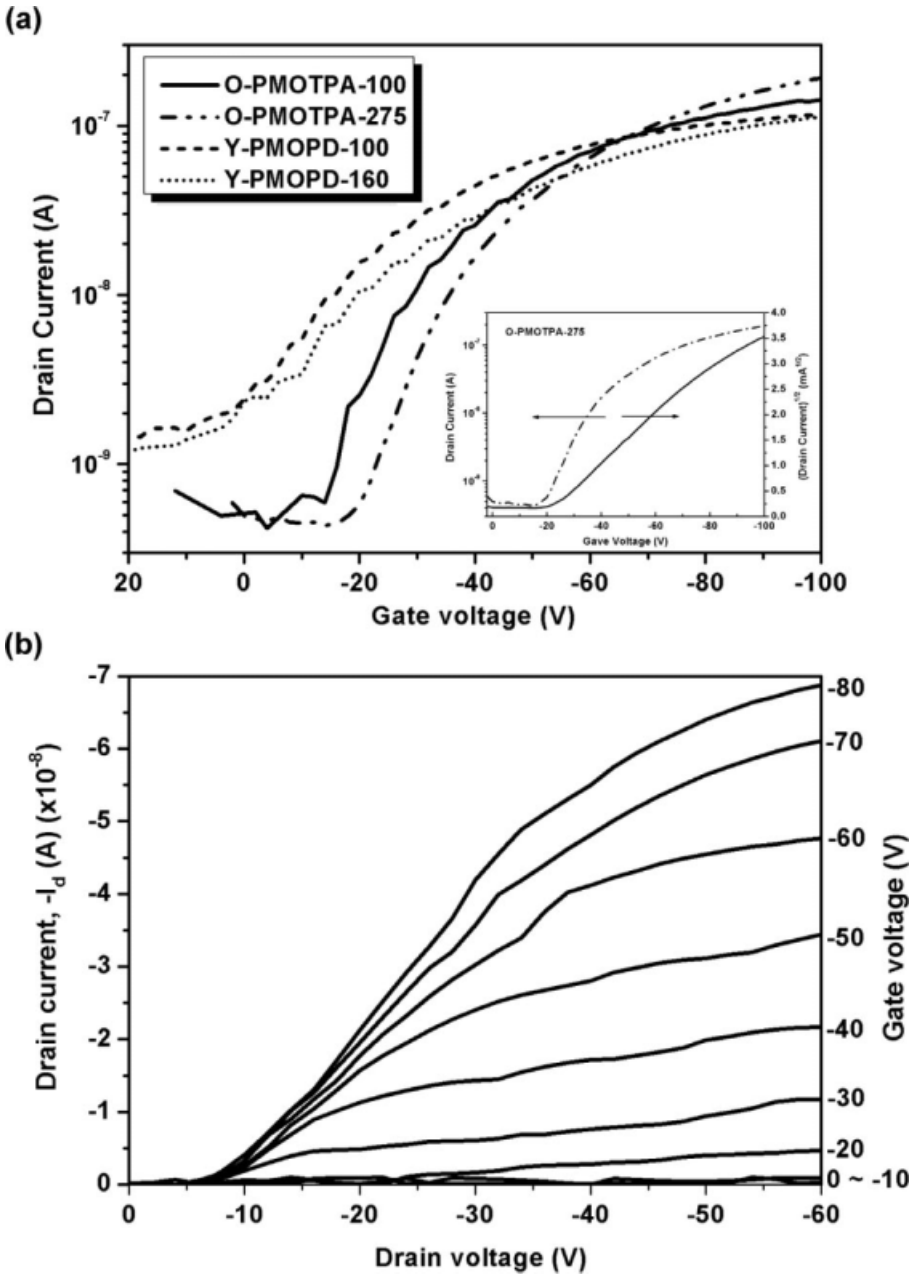

Figure 6. (a) The transfer characteristics of **O-PMOTPA** and **Y-PMOPD** devices, where $V_{ds} = -100$ V; (b) The output characteristic of **O-PMOTPA** baked at 100 °C.

Table 5. OTFT Characteristics of the Studied Polymers

	$CHCl_3$, Annealed at 100 °C for 3 h				$CHCl_3$, Annealed Above T_g for 3 h			
Polymer Code	Mobility ($cm^2\ V^{-1}\ s^{-1}$)	On/Off Ratios	V_t (V)	RMS Roughness (nm)[a]	Mobility ($cm^2\ V^{-1}\ s^{-1}$)	On/Off Ratios	V_t (V)	RMS Roughness (nm)[a]
Y-PMOTPA	5.0E-05	110	−7	0.296	9.0E-05	190	−6	0.775
O-PMOTPA	9.0E-05	340	−11	0.307	1.5E-04[b]	450[b]	−19[b]	2.187
Y-PMOPD	5.6E-05	80	8	0.547	4.0E-05	100	8	0.613

[a] RMS: Root-mean-square.
[b] Only annealed above T_g for 10 min.

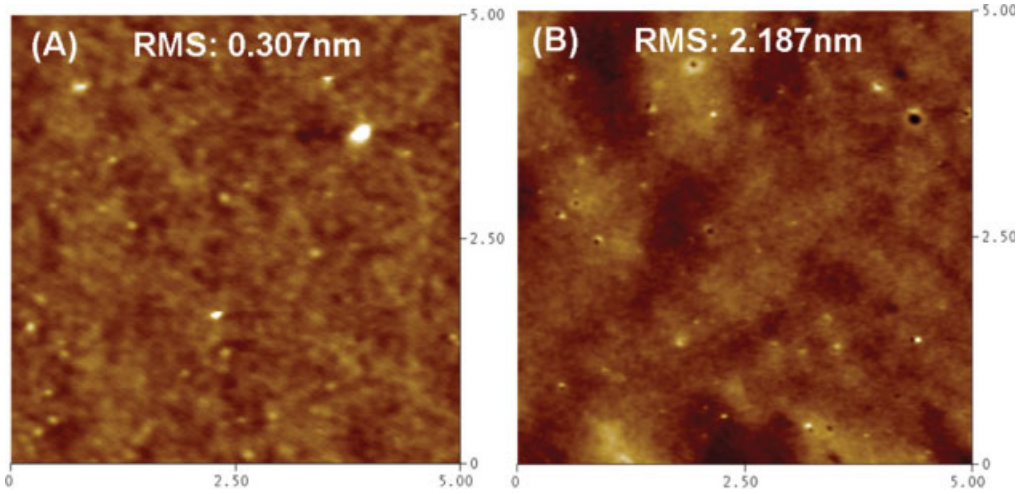

Figure 7. Topographical AFM images of **O-PMOTPA** on OTS-modified SiO_2 surface, under (A) 100 °C and (B) 275 °C heat treatment. The image size is 5 μm × 5 μm. The *Z*-range for (A) is 15 nm and for (B) is 50 nm.

340 and 450, respectively. The hole mobility was increased after device annealed and it was apparently correlated with the surface morphology. After the devices were annealed, the surface roughness obviously increased, especially for the oxidative coupling one, as shown in Figure 7. It revealed that **O-PMOTPA** had some structural rearrangements after annealed and then enhanced the charge transport. When compared with our previous work,[38] we find the hole mobility of **O-PMOTPA** raises almost two order than the previous low molecular weight **PMeOTPA** (M_w: 2000–3000).[38] Also, the order of hole mobility (**O-PMOTPA** > **Y-PMOTPA** > **PMeOTPA**) are consistent with the order of molecular weight. It indicates that the molecular weight plays an important role in the charge mobility. For **Y-PMOPD** (T_g: 152 °C), the estimated hole mobility under 100 and 160 °C treatment is 5.6×10^{-5} and 4.0×10^{-5} $cm^2\ V^{-1}\ s^{-1}$ and the corresponding on/off ratios are 80 and 100. The device performance is similar before and after annealed. The surface morphology without any significant variation also confirms these results (Shown in Supporting Information Fig. S1). The lower mobilities of **PMOPD** than **PMOTPA** obviously originate from the different oxidation position. For **PMOTPA**, the only N atom on the polymer backbone form stable cation after oxidation, which favor to form p-channel. As for **PMOPD**, the first stable cation formed on the side-chain position N atom, which would become a drawer and difficult to form stable p-channel. The above results suggest that the molecular weight, annealing temperature, and polymer structure significantly affect the charge transporting ability.

CONCLUSIONS

Two kinds of soluble polymers containing TPA unit with high fluorescence quantum yield in NMP solution have been successfully synthesized by the various coupling polymerization. These polymers in chloroform solution exhibited PL intensity relatively lower than other solvents, due to the possible photo-oxidation of polymer in the solvent. Similar phenomena led to the higher molecular weight of the **O-PMOTPA** by oxidative coupling polymerization. Attaching bulky and electron-donating TPA units to the polymer main chain and/or as pendent group not only facile the color tuning of the electrochromic behaviors but also disrupts the coplanarity of aromatic units in chain packing. Thus, all of the polymers were amorphous with good solubility in many polar aprotic solvents and exhibited excellent thin film formability. Field effect transistors fabricated from **PMOTPA** series and **PMOPD** showed p-type characteristics. The p-channel carrier mobility up to 1.5×10^{-4} $cm^2\ V^{-1}\ s^{-1}$ was obtained for the **O-PMOTPA-**based FET device. The FET mobility of **PMOTPA** suggested that both the molecular weight and the annealing effects played important roles in charge mobility. This study demonstrates that triphenylamine-containing conjugated polymer is a multifunctional material for various optoelectronic device applications.

REFERENCES AND NOTES

1. Akcelrud, L. Prog Polym Sci 2003, 28, 875–962.
2. Kim, D. Y.; Cho, H. N.; Kim, C. Y. Prog Polym Sci 2000, 25, 1089–1139.
3. Tao, X. T.; Zhang, Y. D.; Wada, T.; Sasabe, H.; Suzuki, H.; Watanabe, T.; Miyata, S. Adv Mater 1998, 10, 226–230.
4. (a) Hou, J.; Yang, C.; He, C.; Li, Y. Chem Commun 2006, 871–873; (b) Hou, J.; Tan, Z.; Yan, Y.; He, Y.; Yang, C.; Li, Y. J. J Am Chem Soc 2006, 128, 4911–4916; (c) Li, Y.; Zou, Y. Adv. Mater 2008, 20, 2952–2958.
5. Muccini, M. Nat Mater 2006, 5, 605–613.
6. Yu, L.; Chan, W. K.; Peng, Z.; Gharavi, A. Acc Chem Res 1996, 29, 13–21.
7. Ranger, M.; Rondeau, D.; Leclerc, M. Macromolecules 1997, 30, 7686–7691.
8. Yamamoto, T.; Morita, A.; Muyazaki, Y.; Maruyama, T.; Wakayama, H.; Zhou, Z. H.; Nakamura, Y.; Kanbara, T.; Sasaki, S.; Kubota, K. Macromolecules 1992, 25, 1214–1223.
9. Lin, H. Y.; Liou, G. S. J Polym Sci Part A: Polym Chem 2009, 47, 285–294.
10. Naarman, H.; Theophilou, N. Synth Met 1987, 22, 1–8.
11. Daoust, G.; Leclerc, M. Macromolecules 1991, 24, 455–459.
12. Grem, G.; Leditzky, G.; Ullrich, B.; Leising, G. Adv Mater 1992, 4, 36–37.
13. Pei, Q.; Yang, Y. J Am Chem Soc 1996, 118, 7416–7417.
14. Scherf, U.; Mullen, K. Makromol Chem Rapid commun 1991, 12, 489–497.
15. Yamamoto, T. Bull Chem Soc Jpn 1999, 72, 621–638.
16. Son, J. M.; Mori, T.; Ogino, K.; Sato, H.; Ito, Y. Macromolecules 1999, 32, 4849–4854.
17. Ogino, K.; Kanegae, A.; Yamaguchi, R.; Sato, H.; Kurjata, J. Macromol Rapid Commun 1999, 20, 103–106.
18. Wu, A.; Kakimoto, M. Adv Mater 1995, 7, 812–814.
19. Wu, A.; Jikei, M.; Kakimoto, M.; Imai, Y.; Ukishima, Y. S.; Takahashi, Y. Chem Lett 1994, 23, 2319–2322.
20. (a) Van der Auweraer, M.; De Schryver, F. C.; Borsenberger, P. M.; Fitzgerald, J. J. J Phys Chem 1993, 97, 8808–8811; (b) Park, M. H.; Huh, J. O.; Do, Y.; Lee, M. H. J Polym Sci Part A: Polym Chem 2008, 46, 5816–5825.
21. Naito, K.; Miura, A. J Phys Chem 1993, 97, 6240–6248.
22. Yang, Y.; Pei, Q.; Heeger, A. J. J Appl Phys 1996, 79, 934–939.
23. Louie, J.; Hartwig, J. F.; Fry, A. J. J Am Chem Soc 1997, 119, 11695–11696.
24. Chiu, K. Y.; Su, T. H.; Huang, C. W.; Liou, G. S.; Cheng, S. H. J Electroanal Chem 2005, 578, 283–287.
25. Bonvoisin, J.; Launay, J. P.; Rovira, C.; Veciana, J. Angew Chem Int Ed Engl 1994, 33, 2106–2133.
26. (a) Huo, L.; He, C.; Han, M.; Zhou, E.; Li, Y. J Polym Sci Part A: Polym Chem 2007, 45, 3861–3871; (b) Huo, L.; Tan, Z.; Wang, X.; Han, M.; Li. Y. Synth Met 2007, 157, 690–695.
27. Chiu, K. Y.; Su, T. H.; Li, J. H.; Lin, T. H.; Liou, G. S.; Cheng, S. H. J Electroanal Chem 2005, 575, 95–101.
28. Liou, G. S.; Chang, H. W.; Lin, K. H.; Su, Y. L. O. J Polym Sci Part A: Polym Chem 2009, 47, 2118–2131.
29. Chou, M. Y.; Leung, M. K.; Su, Y. O.; Chiang, S. L.; Lin, C. C.; Liu, J. H.; Kuo, C. K.; Mou, C. Y. Chem Mater 2004, 16, 654–661.
30. (a) Liou, G. S.; Chang, C. W. Macromolecules 2008, 41, 1667–1674; (b) Liou, G. S.; Lin, H. Y. Macromolecules 2009, 42, 125–134; (c) Chang, C. W.; Yen, H. J.; Huang, K. Y.; Yeh, J. M.; Liou, G. S. J Polym Sci Part A: Polym Chem 2008, 46, 7937–7949.
31. Creutz, C.; Taube, H. J Am Chem Soc 1973, 95, 1086–1094.
32. Lambert, C.; Noll, G. J Am Chem Soc 1999, 121, 8434–8442.
33. Leung, M. K.; Chou, M. Y.; Su, Y. O.; Chiang, C. L.; Chen, H. L.; Yang, C. F.; Yang, C. C.; Lin, C. C.; Chen, H. T. Org Lett 2003, 5, 839–842.
34. Bailey, S. E.; Zink, J. I.; Nelsen, S. F. J Am Chem Soc 2003, 125, 5939–5947.
35. Robin, M.; Day, P. Adv Inorg Radiochem 1967, 10, 247–422.
36. Szeghalmi, A. V.; Erdmann, M.; Engel, V.; Schmitt, M.; Amthor, S.; Kriegisch, V.; Noll, G.; Stahl, R.; Lambert, C.; Leusser, D.; Stalke, D.; Zabel, M.; Popp, J. J Am Chem Soc 2004, 126, 7834–7845.
37. Marken, F.; Hayman, C. M.; Bulman Page, P. C. Electrochem Commun 2002, 4, 462–467.
38. Liou, G. S.; Yang, Y. L.; Chen, W. C.; Su, Y. L. O. J Polym Sci Part A: Polym Chem 2007, 45, 3292–3302.
39. Shi, W.; Fan, S.; Huang, F.; Yang, W.; Liu, R.; Cao, Y. J Mater Chem 2006, 16, 2387–2394.
40. Cho, H. J.; Jung, B. J.; Cho, N. S.; Lee, J.; Shim, H. K. Macromolecules 2003, 36, 6704–6710.
41. Sim, J. H.; Yamada, K.; Lee, S. H.; Yokokura, S.; Sato, H. Synth Met 2007, 157, 940–944.
42. Ueda, M.; Hayakawa, T.; Haba, O. Macromolecules 1997, 30, 7069–7074.
43. Fitzgerald, E. A.; Wuelfing, P.; Richtol, H. H. J Phys Chem 1971, 75, 2737–2741.
44. Petrushenko, K. B.; Kylba, L. V.; Smirnow, V. I.; Shevchenko, S. G. Russ Chem Bull 2001, 50, 798–804.
45. Kong, X. X.; Kulkarni, A. P.; Jenekhe, S. A. Macromolecules 2003, 36, 8992–8999.
46. Horowitz, G. Adv Mater 1998, 10, 365–377.